Stator Current Signature Analysis of Healthy Induction Motor Using Time Stepping Finite Element Method

Noura Halem[1], Kamel Srairi[1], and Salah Eddine Zouzou[2]

[1]Université de Biskra, Laboratoire de Modélisation des Systèmes Energétiques (*LMSE*), Biskra, ALGERIA
[2]Université de Biskra, Laboratoire de Génie Electrique (*LGEB*), Biskra, ALGERIA
noura.halem@yahoo.fr, ksrairi@yahoo.fr

Abstract: Application of *MCSA* for diagnosis of induction motors requires a well previously knowledge of various frequency components in stator current spectrum of motor in healthy state. This paper takes a closer look on healthy stator current spectrum content, which offers an important new contribution to enrich the most famous technique of fault diagnosis of induction motors. In aim to assure the obtaining of high space harmonics of motor, the *TSFEM* is used to model the healthy induction motor. The rotor and stator slotting are taken into account. Moreover, the paper reports an investigation about the magnetic saturation influence on the content of healthy stator current spectrum, for this purpose the *linear* and *non-linear permeability* are included in induction motor model. In order to show the impact of varying load on the healthy stator current spectrum content, the simulation results are extracted at different loads.

Keywords: Induction motor; time stepping finite element method (*TSFEM*); magnetic saturation; linear-permeability; non-linear permeability; electromagnetic field; motor current signature analysis (*MCSA*); harmonics

Abbreviations list:
TSFEM: Time Stepping Finite Elements Method
MCSA: Motor Current Signature Analysis
FFT: Fast Fourier Transform
PSHs: Principal Slot Harmonics
PSH1: Lower (First) Principal Slot Harmonic
PSH2: Upper (Second) Principal Slot Harmonic

1. Introduction

Nowadays, motor current signature analysis (*MCSA*) is a popular technique for diagnosis of different defaults in induction motor [1]-[2]-[3]. *MCSA* technique is based on the detection of new generated frequency components in stator current spectrum, or in some cases by the amplitudes varying of old frequency components in current spectrum. In the both cases, a well knowledge of stator current spectrum content in healthy state is strongly required for a reliable diagnosis of induction motor defaults.

Frequently, induction motors are modeled with negligence of many important phenomena in motor, such as magnetic saturation of lamination core, rotor and stator notching [4]-[5]. It is not the real case, which affects directly on the spaces harmonics of motor. So the consequence that the following frequency components are surely missing in the stator current spectrum [5]:

- Saturation harmonics (causing by the use of permeability independent of time),
- Rotor slot harmonics.

Really few methods of induction motor modeling, can offer a high space harmonics, which allow a restful application of *MCSA*. One of the most precise modeling methods; is the finite element method, which plays an important role in assisting the analysis of induction motor [6]-[7]-[8].

Received: December 7th, 2013. Accepted: February 26th, 2014

TSFEM is the most precise way to conserving the electromagnetic behavior of induction motor. The central point in the *TSFEM* is the determination of magnetic field by the nonlinear *TSFEM*, the magnetic force and torque are calculated by using the Maxwell stress tensor. The mechanical motion is solver by a numerical method. After the mechanical equation determines the new angular and radial position of a rotor, the finite element model is rearranged to recalculate the magnetic field by moving mesh technique [5]-[9]-[10]. From many models based on finite elements method, only the circuit-coupled finite element technique can closes the real life of induction motors, here the magnetic circuit of motor is coupled with the external electric circuit excited by sinusoidal voltage source [11].

As the magnetic saturation is an invariant phenomenon in induction motors, this paper reports an important investigation of saturation magnetic effect on healthy stator current spectrum content by comparing the unsaturated and saturated stator current spectrums. Impact of varying load on default index signatures is treated by several researches [12]. However it will be rigorous to keeping information about the influence of varying loads on the harmonics of healthy stator spectrum before heading to use *MCSA*.

The purpose of this study is to make an extensive look about what can healthy stator current spectrum contains, as a first step for diagnosis of induction motor defaults using *MCSA*.

In Section 2 of this paper, the healthy induction motor will be modeled using *TSFEM*. Section 3 deals with analysis of healthy stator current spectrum of unsaturated and saturated induction motor at different loads.

2. Modeling of healthy induction motor using TSFEM

In this paper, induction motor under healthy state is modeled using *TSFEM* through the circuit-coupled finite element technique. The external electric circuit of stator and rotor which presented in figure 2 is coupled with the finite element domain as presented in figure 3. Figure 1 presents the model of induction motor. Table 1 presents the specific characteristics of induction motor.

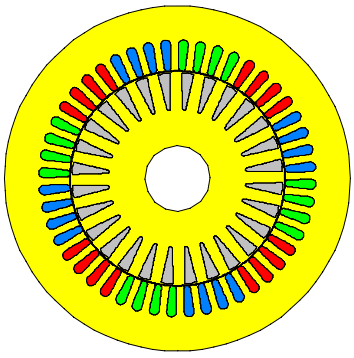

Figure 1. Induction motor model

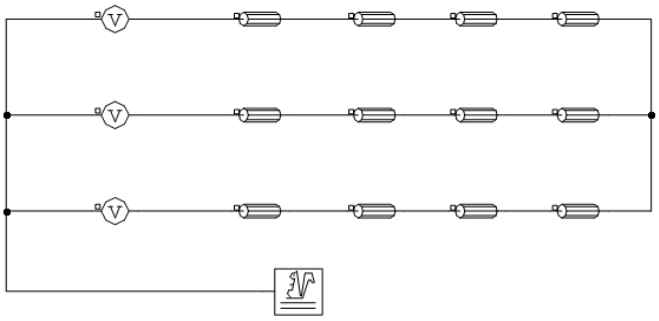

Figure 2. External electric circuit model

Table 1. Specifications of studied induction motor

Variable	Value
Number of poles	4
Number of phases	3
Rated power (*kW*)	1.1
Rated voltage (*V*)	230
Frequency (*Hz*)	50
Rated speed (*rpm*)	1425
Number of stator slots	36
Number of rotor slots	28

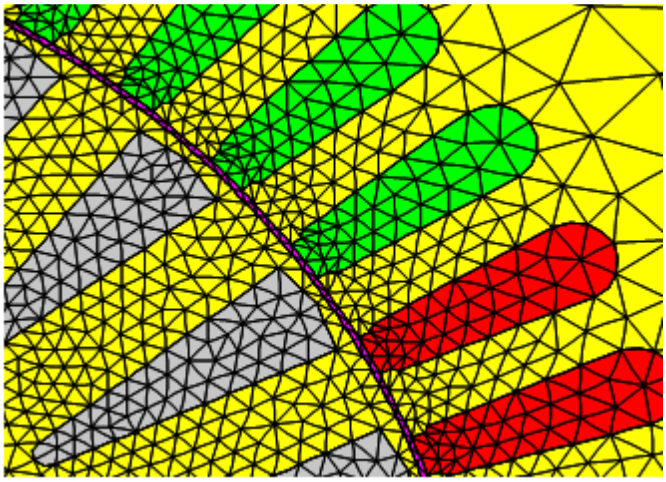

Figure 3. Finite element domain

The transient magnetic field in terms of magnetic vector potential A, ν the reluctivity, conductivity σ, and current density J can be expressed as [10]:

$$\frac{\partial}{\partial x}\left(\nu\frac{\partial A}{\partial x}\right)+\frac{\partial}{\partial y}\left(\nu\frac{\partial A}{\partial y}\right)=-J+\sigma\frac{\partial A}{\partial t} \quad (1)$$

The last term represents current induced in conducting material when flux changes with time.

The transient performance is obtained by accounting for the mechanical equation of the motor and the transient motional induced eddy current in the massive conductors can't be neglected as in equation (1), the complete system is based on the differential equation in compact form:

$$\nu\times\left(\nu\nabla\times A\right)=\sigma\left[-\frac{\partial A}{\partial t}-\nabla E+V\times\left(\nu\times A\right)\right] \quad (2)$$

Where *V* is the speed of the rotor, *E* is the electrical scalar potential applied by the external circuit. The problem is considered as transient alike. When the motor is loaded the voltage time step must be accompanied by rotor motion corresponding to the slip [10]-[13]-[14].

The time step must be sufficiently small to ensure that the effects of slotting are accurately modeled, also to obtain a suitable frequency resolution for the application of *FFT* [1]-[5].

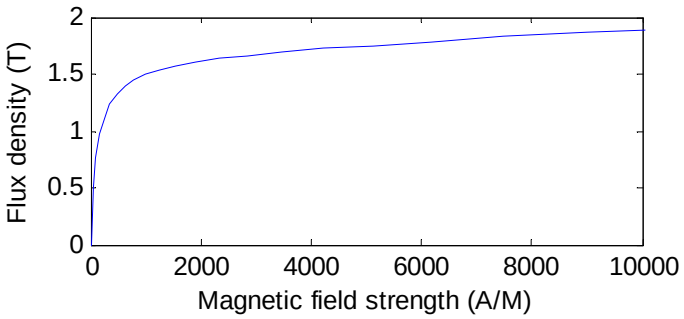

Figure 4. Proposed magnetic characterization

An initial iron relative permeability of 1000 is assigned to the ferromagnetic core. Then, the calculations are done for a saturated ferromagnetic material by a *B-H* curve (figure 4).

3. Spectrum analysis of stator current in healthy induction motor

The frequencies given by (3) are used to detect eccentricity-related fault signatures in the stator current. f_s is the fundamental supply frequency, R is the number of rotor slots, s is the slip, p is the number of pole pairs, and λ is the order of the stator time harmonics that are present in motor current spectrum $(\lambda = \pm 1, \pm 3, \pm 5, ...)$ [15]-[16].

$$f_h = \left[\left(k\,R \pm n_d \right) \frac{(1-s)}{p} \pm \lambda \right] f_s \tag{3}$$

- In case of *static eccentricity*: $n_d = 0$, $k = 1, 2, 3, \ldots$.
- In case of *dynamic eccentricity*: $k = 0$, $n_d = 1, 2, 3, \ldots$ (n_d is known as eccentricity order).
- In case of *mixed eccentricity*: $n_d = 1, 2, 3, \ldots$, $k = 1, 2, 3, \ldots$.
- In case of *healthy state*: $k = 0$, $n_d = 0$.

$$f_h = \left| \lambda f_s \pm R f_r \right| \tag{4}$$

$$f_r = \frac{(1-s)}{p} f_s \tag{5}$$

The appearing of new frequency components around principal slot harmonics (*PSHs*), also the variation of its amplitude values are frequently used to diagnose some faults in induction motors such as eccentricity default.

PSHs are given by the following relationships [16]-[17]:

- The lower (first) principal harmonic:

$$f_{PSH1} = \left| f_s - R\, f_r \right| \tag{6}$$

- The upper (second) principal harmonic:

$$f_{PSH2} = \left| f_s + R\, f_r \right| \tag{7}$$

Figure 5 shows the stator current spectrum for healthy loaded four-pole induction motor with *S*=36 stator slots and *R*=28 rotor bars at *s*=4.8%, under linear permeability. The two *PSHs* exist in the spectrum at: $\left| f_s \pm R\, f_r \right| = \left| 50 \pm 28\left(\left(1 - 0.048 \right) 50/2 \right) \right| = 616.4\ Hz$ and $716.4\ Hz$. Obviously the amplitude of *PSH1* (-63.33 *dB*) is very larger than the amplitude of *PSH2* (-63.33 *dB*). As predictable, except *PSHs* all of rotor slot and time harmonics are missing.

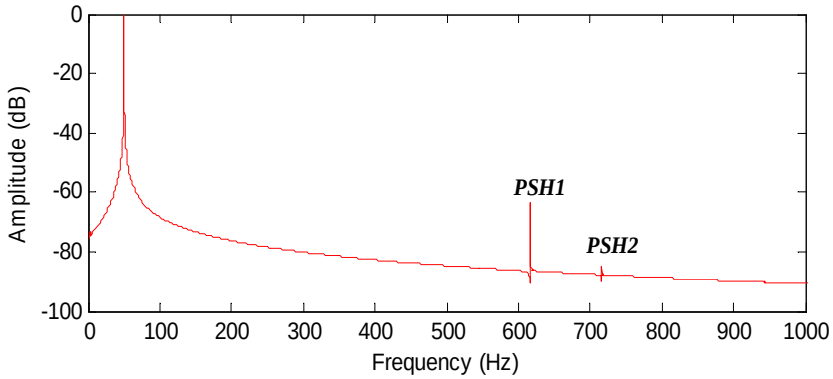

Figure 5. Simulated stator current spectrum for healthy unsaturated induction motor at full-load, *S*=36, *R*=28, *p*=2 pole pairs, *s*=4.8%

Figures 6, 7 and 8 present the stator current spectrum for healthy loaded four-pole induction motor with *S*=36 stator slots and *R*=28 rotor bars at *s*=4.8%, under non-linear permeability. According predictions, all the expected frequency components are clearly appearing in the spectrums (figures 6, 7 and 8); these harmonics can be classified as following:

- The two *PSHs* are existed at:

$$\left| f_s \pm R\, f_r \right| = \left| 50 \pm 28\left(\left(1 - 0.0483 \right) 50/2 \right) \right| = 616.2\ Hz \text{ and } 716.2\ Hz.$$

- As expected, when magnetic saturation is taken into account, the whole series of saturation-related harmonics result of magnetic saturation are generated such as:

$$\left| 3 f_s \pm R\, f_r \right| = \left| 3 \cdot 50 \pm 28\left(\left(1 - 0.0483 \right) 50/2 \right) \right| = 516.2\ Hz \text{ and } 816.2\ Hz.$$

$$\left| 5 f_s \pm R\, f_r \right| = \left| 5 \cdot 50 \pm 28\left(\left(1 - 0.0483 \right) 50/2 \right) \right| = 416.2\ Hz \text{ and } 916.2\ Hz.$$

- Even under balanced power supply and in symmetrical conditions, the component at 150 *Hz* is generated. Also the fifth (250 *Hz*) and seventh (350 *Hz*) harmonics are existed in the current spectrum. The appearing of fifth and seventh current time harmonics is due to the

voltage time harmonics in the supply voltages. However, as known the appearing of these harmonics is due to the saturation of the main magnetic flux path [17]-[18].

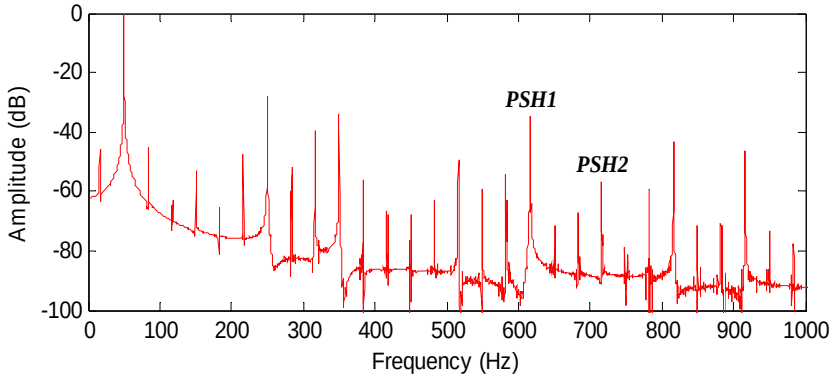

Figure 6. Simulated stator current spectrum for healthy saturated induction motor at full-load, S=36, R=28, p=2 pole pairs, s=4.83

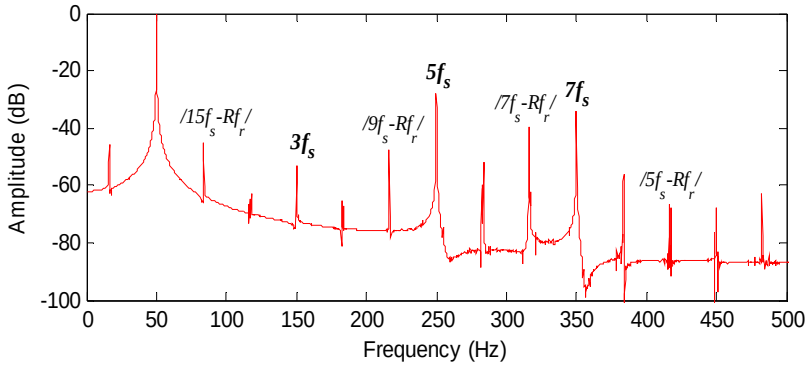

Figure 7. Simulated stator current spectrum for healthy saturated induction motor at full-load, S=36, R=28, p=2 pole pairs, s=4.83%, (0-500 Hz)%

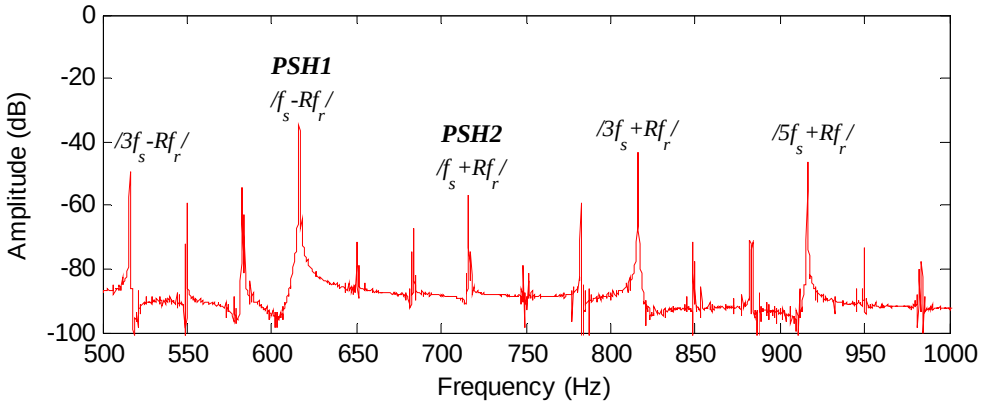

Figure 8. Simulated stator current spectrum for healthy saturated induction motor at full-load, S=36, R=28, p=2 pole pairs, s=4.83%, (500-1000 Hz)

In order to show the impact of varying loads on the content of healthy stator current spectrum, figures 9 and 10 show respectively the stator current spectrum for healthy saturated induction motor at half-load and no-load.

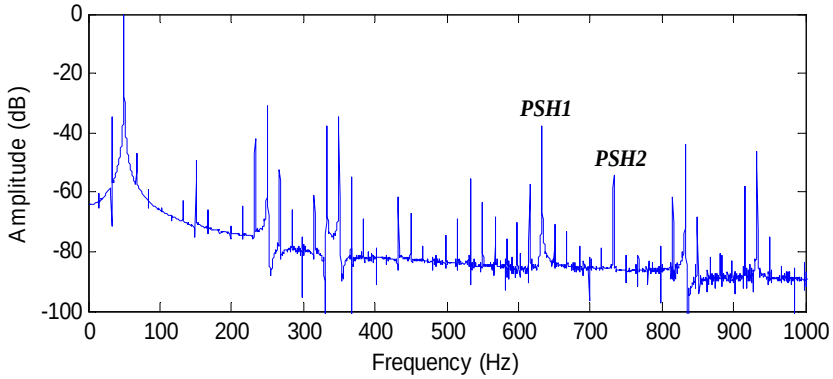

Figure 9. Simulated stator current spectrum for healthy saturated induction motor at half-load, S=36, R=28, p=2 pole pairs, s=2.44%

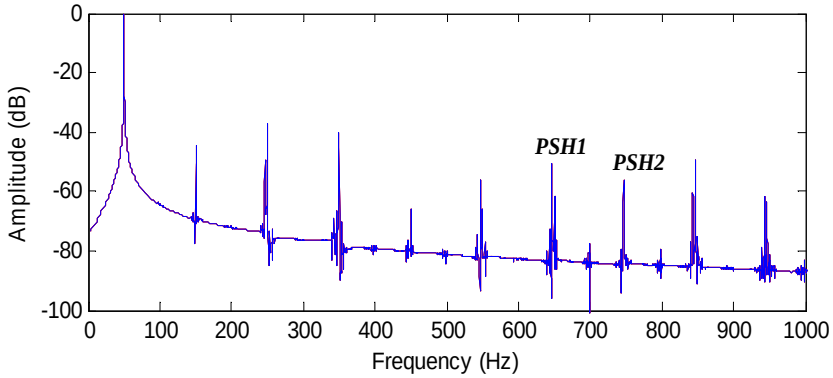

Figure 10. Simulated stator current spectrum for healthy saturated induction motor at no-load, S=36, R=28, p=2 pole pairs, s=0.48%

As shown in figures 9 and 10, the frequencies given by (6) and (7) depend on motor load, by other words; position of *PSHs* in stator current spectrum depends on rotor speed.
Such as an example, in figure 9 when the motor is at half-load the *PSHs* occur at: $\left| f_s \pm R\ f_r \right| = \left| 50 \pm 28\left(\left(1 - 0.0244 \right) 50/2 \right) \right| = 632.92\ Hz$ and $732.92\ Hz$.

At no-load (figure 10) *PSHs* occur at: $\left| f_s \pm R\ f_r \right| = \left| 50 \pm 28\left(\left(1 - 0.0048 \right) 50/2 \right) \right| = 646.64\ Hz$ and $646.64\ Hz$. However, the existence of *PSHs* in current spectrum depends on the number of pole pairs and rotor slots which lead that the detection of fault in stator current spectrum around the *PSHs* is effective only for some combination of number of pole pairs and rotor slots [17]-[18].

Table 2. Amplitude of saturation-related harmonics and *PSHs* components for healthy saturated induction motor at different loads in *dB*

Saturation-related harmonics and *PSHs* $\lvert\lambda f_s \pm R f_r\rvert$	Frequency (*Hz*) at full-load	Full-load	Half-load	No-load
$\lvert 13 f_s - R f_r\rvert$	16.2	-47.34	-34.74	0
$\lvert 11 f_s - R f_r\rvert$	116.2	-42.08	-62.77	0
$\lvert 9 f_s - R f_r\rvert$	216.2	-46.72	-42.26	-49.39
$\lvert 7 f_s - R f_r\rvert$	316.2	-40.20	-38.04	-66.79
$\lvert 5 f_s - R f_r\rvert$	416.2	-42.08	-61.82	-76.57
$\lvert 3 f_s - R f_r\rvert$	516.2	-49.82	-55.55	-56.06
$\lvert f_s - R f_r\rvert$ *PSH1*	616.2	-33.12	-37.73	-50.90
$\lvert f_s + R f_r\rvert$ *PSH2*	716.2	-30.56	-54.37	-55.92
$\lvert 3 f_s + R f_r\rvert$	816.2	-37.47	-43.93	-49.62
$\lvert 5 f_s + R f_r\rvert$	916.2	-46.20	-46.57	-63.53

Table 3. Amplitude of time harmonics components for healthy saturated induction motor at different loads in *dB*

Time harmonics λf_s	Frequency (*Hz*)	Full-load	Half-load	No-load
$3 f_s$	150	-52.93	-49.17	-44.32
$5 f_s$	250	-27.79	-31.14	-37.02
$7 f_s$	350	-33.96	-34.59	-40.12
$9 f_s$	450	-67.72	-67.40	-65.09
$11 f_s$	550	-59.22	-63.49	-66.24
$13 f_s$	650	-71.40	-70.82	-61.72
$15 f_s$	750	-81.45	-81.58	-83.19
$17 f_s$	850	-77.61	-68.24	-74.86
$19 f_s$	950	-73.15	-75.06	-85.64

Table 2 and 3 summarize respectively the amplitude values of saturation-related harmonics and time harmonics. Obviously, varying of loads affects strongly on the amplitude values of saturation-related harmonics of healthy stator current spectrum, such as the amplitude of frequency components *PSH2* is decreased from -30.56 *dB* at full-load to -54.37 *dB* at half-load. While the amplitude values of time harmonics are touched by low variations when the load varied.

On the other side, according to figures 9 and 10, it can be shown that varying of load do not affect only on position of harmonics and its amplitude values. Moreover, varying of load affects on appearing of frequency components in healthy stator current spectrum, as summarized in tables 2 and 3 some of saturation-related harmonics are missing when the motor is at no-load.

It must note that in some cases, when induction motor suffered from defect such as purely static eccentricity, no fault index can clearly appear in stator current spectrum [8]; just perturbation of amplitude values can be shown in previously prominent harmonics such as *PSHs* and saturation-related harmonics. Even with small default degree of a previously knowledge of amplitude values of harmonics in healthy stator current spectrum, can help to detect any perturbation in the motor.

4. Conclusion

In this paper, a highly precise modeling using *TSFEM* is proposed to analysis precisely the stator current spectrum of healthy induction motor as a preparatory step before using *MCSA* to diagnose defects in induction motors. It was shown that the magnetic saturation injected saturation-related and time harmonics which recognized as the most prominent harmonics induction motors. In this paper, the stator current spectrums have been extracted at different loads to verify the impact of varying load on amplitude values of harmonics.

Acknowledgement

The authors would like to thank Professor Champenois at the LAII laboratory, Poitiers, France, for his help.

References

[1] W. T. Thomson and A. Barbour, "On-line current monitoring and application of finite element method to predict the level of static airgap eccentricity in three-phase induction motors", *IEEE Trans. Energy. Convers, vol. 13, no. 4, pp. 347-357, 1998.*

[2] M. E. H. Benbouzid and G. B. Kliman, "What stator current processing-based technique to use for induction motor rotor faults diagnosis?", *IEEE Trans. Energy Convers, vol. 18, no. 2, pp. 238-244, Jun. 2003*.

[3] N. Feki, G. Clerc, and Ph. Velex , "Gear and motor fault modeling and detection based on motor current analysis", *Electric Power Systems Research, vol. 95, pp: 28-37, 2013*.

[4] J. Faiz, B. M. Ebrahimi, and H. A. Toliyat, "Effect of magnetic saturation on static and mixed eccentricity fault diagnosis in induction motor," *IEEE Trans Magnetics, vol. 45, no. 8, pp 3137-3144, 2009*.

[5] A. B. J. Reece and T.W. Preston, "Finite element methods in electrical power engineering," *Oxford Science Publication, 2000*.

[6] J. F. Bangura and N. A. O. Demerdash, "Diagnosis and characterization of effects of broken rotor bars and connectors in squirrel-cage induction motors by a time-stepping coupled finite element-state space modeling approach", *IEEE Trans. Energy Convers, vol. 14, no. 4, pp. 1167-1176, Dec. 1999.*

[7] J. Faiz, B. M. Ebrahimi, B. Akin. H. A. Toliyat, "Comprehensive eccentricity fault diagnosis in induction motors using finite element method", *IEEE Trans. Magnetics. vol. 45, no. 3, pp. 1764-1767, 2009.*

[8] N. Halem, S. E. Zouzou, K. Srairi, S. Guedidi and F. Abood, "Static eccentricity fault diagnosis using the signatures analysis of stator current and air gap magnetic flux by

finite element method in saturated induction motors", *Int J Syst Assur Eng Manag, vol. 4, no. 2, pp. 118–128, Jun. 2013*.

[9] Y. Ouazir, N. Takorabet, R. Ibtiouen and M. Benhaddadi, "Time-stepping FE analysis of cage induction motor with air-gap interface coupling taking into account phase-belt harmonics," *IEEE Trans Magnetics, vol. 45, no. 3, pp 1384-1387, 2009*.

[10] T. W. Preston, A. B. J. Reece and P. S. Sangha, "Induction motor analysis by time-stepping technique", *IEEE Trans Magnetics, vol. 24, no. 1, pp 471-474, 1988*.

[11] N. Sadowski, R. Carlson, S. R. Arruda , C. A. Silva and M. L. Mazenc, "Simulation of single-phase induction motor by general method coupling field and circuit equations", *IEEE Trans Magnetics, vol. 31, no. 3, pp. 1908–1911, 1995*.

[12] J. Faiz, B. M. Ebrahimi, H.A. Toliyat and W.S. Abu-Elhaija, "Mixed-fault diagnosis in induction motors considering varying load and broken bars location", *Energy Conversion and Management, Vol. 51, no. 7, pp. 1432-1441 July 2010*.

[13] S. J. Salon, D. W. Burow, R. E. Ashly, L. Ovacik and M. J. DeBotoli, "Finite element analysis of induction machine in the frequency domain", *IEEE Trans Magnetics, vol. 29, no. 2, pp. 1438–1441, 1993*.

[14] P. Lombard and G. Meunier, "A general method for electric and magnetic coupled problem in 2D and magnetodynamic domain", *IEEE Trans Magnetics, vol. 28, no. 2, pp. 1291-1294, 1992*.

[15] S. Nandi, T. C. Ilamparithi, S. B. Lee, and D. Hyun, "Detection of eccentricity faults in induction machines based on nameplate parameters", *IEEE Trans. Ind. Appl, vol. 58, no. 5, pp. 1673-1683, 2011*.

[16] G. Joksimovic, "Line current spectrum analysis in saturated three-phase cage induction machine", *Electrical Engineering, Springer Verlag, vol. 91, no. 8, pp. 425-437, 2010*.

[17] G. M. Joksimovic, J. Riger, T. M. Wolbank, N. Peric and M. Vasak, "Stator-current spectrum signature of healthy cage rotor induction machines", *IEEE Trans. Magnetics, vol. 60, no. 9, pp. 4025-4033, 2013*.

[18] S. Nandi, "A detailed model of induction machines with saturation extendable for fault analysis", *IEEE Trans. Ind. Appl, vol. 40, no. 5, pp. 1302-1309, 2004*.

Noura HALEM was born in El-oued, Algeria, in 1984. He receives the *B.Sc*. degree in electrical engineering from the University of Biskra, Algeria, in 2007, and the *M.Sc*. degree in electrical networks from the Science and Technology Institute of El-Oued University Center, Algeria, in 2010. She is interested in the modeling, condition monitoring and faults diagnosis of electrical machines and working toward the *Ph. D* degree on the same axis.

Kamel SRAIRI was born in Batna, Algeria, in 1967. He received the *B.Sc.* degree in Electrical Engineering, in 1991, from the University of Batna, Algeria; the *M.Sc.* degree in Electrical and Computer Engineering, from the National Polytechnic Institute of Grenoble, France, in 1992; and the *Ph.D.* degree also in Electrical and Computer Engineering, from the University of Nantes, France, in 1996. After graduation, he joined the University of Biskra, Algeria, where he is a Professor in the Electrical Engineering Department. His main research interests include analysis, design, modeling, optimization and control of electric systems.

Salah Eddine ZOUZOU was born in Biskra, (Algeria) on 1963. He received the *B.S* degree from the "Ecole Nationale Polytechnique d'Alger", Algeria in 1987 and the *M.S* and *Ph.D* degrees from the "École Nationale Polytechnique de Grenoble" France, in 1988 and 1991 respectively. His fields of research interests deal with the design and condition monitoring of electrical machines. He has authored or co-authored more than 50 scientific papers in national and international conferences and journals. Prof. Zouzou is a Professor at the University of Biskra, Algeria and he is the director of the "Laboratoire de Génie Electrique de Biskra" since 2003.